Communicative & Integrative Biology 8:3, e1036206; May/June 2015; Published with license by Taylor & Francis Group, LLC

Cytosolically expressed PrP GPI-signal peptide interacts with mitochondria

Gianni Guizzunti[1,*] and Chiara Zurzolo[2,*]

[1]University of Texas Southwestern Medical Center; Department of Cell Biology; Dallas, TX USA; [2]Institut Pasteur; Unité de Trafic Membranaire et Pathogenèse; Paris, France

We previously reported that PrP GPI-anchor signal peptide (GPI-SP) is specifically degraded by the proteasome. Additionally, we showed that the point mutation P238S, responsible for a genetic form of prion diseases, while not affecting the GPI-anchoring process, results in the accumulation of PrP GPI-SP, suggesting the possibility that PrP GPI-anchor signal peptide could play a role in neurodegenerative prion diseases. We now show that PrP GPI-SP, when expressed as a cytosolic peptide, is able to localize to the mitochondria and to induce mitochondrial fragmentation and vacuolarization, followed by loss in mitochondrial membrane potential, ultimately resulting in apoptosis. Our results identify the GPI-SP of PrP as a novel candidate responsible for the impairment in mitochondrial function involved in the synaptic pathology observed in prion diseases, establishing a link between PrP GPI-SP accumulation and neuronal death.

Keywords: apoptosis, GPI-anchored protein, mitochondria, prion, PrP, signal peptide

Abbreviations: GPI; glycosylphosphatidylinositol; GPI-SP; GPI-anchor signal peptide; ER; endoplasmic reticulum; MMP; mitochondrial membrane potential; FR; folate receptor.

*Correspondence to: Gianni Guizzunti; Email: gianni.guizzunti@gmail.com; Chiara Zurzolo; Email: chiara.zurzolo@pasteur.fr

Submitted: 07/02/2014

Accepted: 07/24/2014

http://dx.doi.org/10.1080/19420889.2015.1036206

Prion diseases are a family of progressive fatal neurodegenerative diseases of infectious, sporadic or inherited origin, which affect humans and other animals. Central to the pathogenesis is the conversion of a host-encoded prion protein, PrP^{C}, into a misfolded, protease resistant isoform, PrP^{Sc}, which accumulates in the brain and constitutes the infectious agent responsible for the disease.[1] Prion diseases are typically diagnosed by manifestation of dementia and locomotor symptoms, which correlate with extensive neuronal loss and PrP^{Sc} deposition. At the histological level, neuronal loss is preceded by synaptic pathology[2-6] and early synaptic failure is a well-documented component of prion diseases.[7,8] However, little is known about the underlying mechanisms of synaptic degeneration, and the sequence of events involved in the neurodegeneration is not yet completely understood.

It has been proposed that impairment in mitochondrial function could be responsible for the synaptic pathology observed in prion diseases. By investigating a wide range of mitochondrial parameters, it was shown that mitochondrial function was impaired in prion diseases and that mitochondrial damage could potentially be the initial cause of synaptic pathology.[9,10] Additionally, several neurodegenerative diseases marked by the accumulation of misfolded proteins, such as Alzheimer and Parkinson diseases, are associated with synaptic dysfunction and mitochondrial abnormalities.[11-14] Evidence that mitochondria could have a role in prion pathology comes from the finding that PrP can interact with neuronal mitochondria and impair their function.[15,16] In transgenic mice overexpressing PrP^{C}, the prion protein localizes to the mitochondria and has been implicated in neuronal apoptosis.[17] Redistribution of PrP^{C} to the mitochondria induces the loss of mitochondrial membrane potential (MMP) and cytochrome c release, resulting in caspase-3-dependent apoptosis, predominantly in hippocampal neurons. Moreover, the expression of PrP^{C} as a cytosolic protein induces the formation of cytosolic aggregates, mitochondrial clustering and promotes cell death by a process that involves depolarization of the mitochondrial membrane, release of

cytochrome c and caspase activation.[18] Finally, the synthetic peptide PrP-(106–126), which has been shown to be neurotoxic,[19] can induce the rapid depolarization of mitochondrial membranes,[20] cytochrome c release and apoptosis in a panel of different neuronal cells.[21,22] While the mechanism of prion disease development remains unclear, mitochondrial damage and dysfunction has emerged as the possible initial cause of synaptic degeneration, which eventually results in apoptotic neuronal cell death. The possibility that the mitochondria constitute the primary site of the proapoptotic pathway opens up new avenues for early diagnosis and particularly for early treatment.

PrP is a glycoprotein that localizes to the plasma membrane via a C-terminally linked glycosylphosphatidylinositol (GPI) anchor.[23] This posttranslational modification concerns over 100 different proteins in humans, including adhesion molecules, surface receptors and enzymes.[24] GPI anchor addition occurs in the lumen of the endoplasmic reticulum (ER), where the pre-assembled GPI anchor is transferred to the acceptor amino acid (called the omega site) by the action of a multimeric GPI transamidase.[25] The GPI transamidase recognizes a C-terminal GPI-anchor signal peptide (GPI-SP), which is cleaved concomitantly to the attachment of the GPI-anchor. The GPI-SP consists of a hydrophilic region (5–10 amino acids) followed by a hydrophobic sequence (15–20 amino acids), but overall lacks a well-defined consensus sequence.[26] As such, they are not usually conserved across species, with the significant exception of PrP, whose GPI-SP shows a remarkable degree of conservation. Additionally, PrP GPI-SP harbors 2 autosomal dominant pathogenic mutations responsible for genetic forms of prion diseases (M232R and P238S); these mutations are particularly perplexing since the GPI-SP is replaced by a GPI anchor and is absent in the mature prion protein.[27,28]

Because of its unusual level of conservation, and because of the presence of unexplained pathogenic mutations in its sequence, PrP GPI-SP represents an ideal model to address the fate of the GPI-anchor signal peptides. To investigate the metabolism of PrP GPI-SP we recently created a hybrid construct where the C-terminus of GFP had been fused to the GPI-SP of PrP, which had then been linked to the double tag Myc-His via a flexible Gly-Ser linker.[29] As a control, we fused GFP to the GPI-SP of Folate Receptor (FR); the GPI-SPs of FR and PrP have the same length (24 amino acids) and an identical size of the hydrophilic (9 amino acids) and the hydrophobic (14 amino acids) regions. We were able to show that, while FR GPI-SP was retained within the lumen of the ER, PrP GPI-SP was selectively transported to the cytoplasm, where it was targeted for degradation by the proteasome. Interestingly, when the pathogenic point mutation P238S was introduced into our construct, PrP GPI-SP was spared from degradation. Linking the P238S point mutation to the accumulation of PrP GPI-SP potentially establishes a link between the accumulation of PrP GPI-SP and PrP induced neurodegeneration, opening up the possibility that PrP GPI-SP could play a role in prion diseases. Here we have investigated the intracellular localization of cytosolic PrP GPI-SP. We show that, differently form the control GPI-SP of Folate Receptor, the GPI-SP of PrP is targeted to the mitochondria, and causes their fragmentation and loss of MMP.

Results and Discussion

To further explore the function of PrP GPI-SP, we decided to investigate the fate of PrP GPI-SP following its retrotranslocation into the cytoplasm. Because the retrotranslocation of proteins into the cytosol is ubiquitination-dependent,[30] we reasoned that the expression of a cytosolic form of PrP GPI-SP (cPrPGPI-SP) would allow PrP GPI-SP to escape ubiquitination. Indeed, it has been shown that ER proteins that are targeted for proteasomal degradation accumulate in the cytosol when degradation is prevented by proteasome inhibitors (as is the case for PrP GPI-SP[29]), but remain restricted to the lumen of the ER under ubiquitination-deficient conditions, confirming that the release of the protein into the cytosol is linked to ubiquitination.[31,32]

The cytosolic versions of PrP's and FR's GPI-SPs (cPrPGPI-SP and cFRGPI-SP respectively) were cloned starting from GFP-FR-MH and GFP-PrP-MH (described in ref. Twenty-nine). In both constructs the GPI-SP was linked to a Myc-His (MH) tag via a Gly-Ser flexible linker, as described in ref. Twenty-nine.

The scheme in **Figure 1**a represents the starting construct (GFP-GPI-tag) and circled in red is the part expressed as cytosolic protein. The constructs were expressed in HeLa cells and analyzed by Western Blot (WB) and immunofluorescence (IF). WB showed that both constructs produced a single band at the expected molecular weight (**Fig. 1b**); by IF analysis, the 2 constructs showed significantly different localization patterns. cFRGPI-SP appeared to localize to a reticular network that extended across the cytoplasm and around the nucleus (**Fig. 1c**), most likely representing the ER. This localization is not surprising, as the hydrophobic region of GPI-SPs can potentially function as an ER-signal sequence, explaining why cFRGPI-SP localizes to the ER. Specifically, PrP GPI-SP has been shown to work as an ER-signal sequence when linked to the N-term of GFP.[33] However, when expressed in HeLa cells, cPrP-GPI-SP localized to discrete tubular elements (**Fig. 1d**), reminiscent of the mitochondrial network. To confirm the localization of our constructs, cells expressing cFRGPI-SP were co-stained with the ER marker Calnexin (**Fig. 1e–g**) and cells expressing cPrPGPI-SP were labeled with the mitochondrial marker Tom20 (**Fig. 1h–j**). As shown in **Figure 1e–j**, complete colocalization confirmed that cPrPGPI-SP localizes to the mitochondria, whereas cFRGPI-SP localizes to the ER.

While cFRGPI-SP ER localization had no effect on the structure of the compartment or on the viability of the transfected cells (data not shown), we noticed that in cells expressing cPrPGPI-SP the mitochondria were affected in a time-dependent fashion: within the first hours after transfection, cPrPGPI-SP localized to intact active mitochondria, as shown by costaining with MitoTracker Red CMXRos. MitoTracker Red CMXRos was used to indicate the alteration of mitochondrial membrane

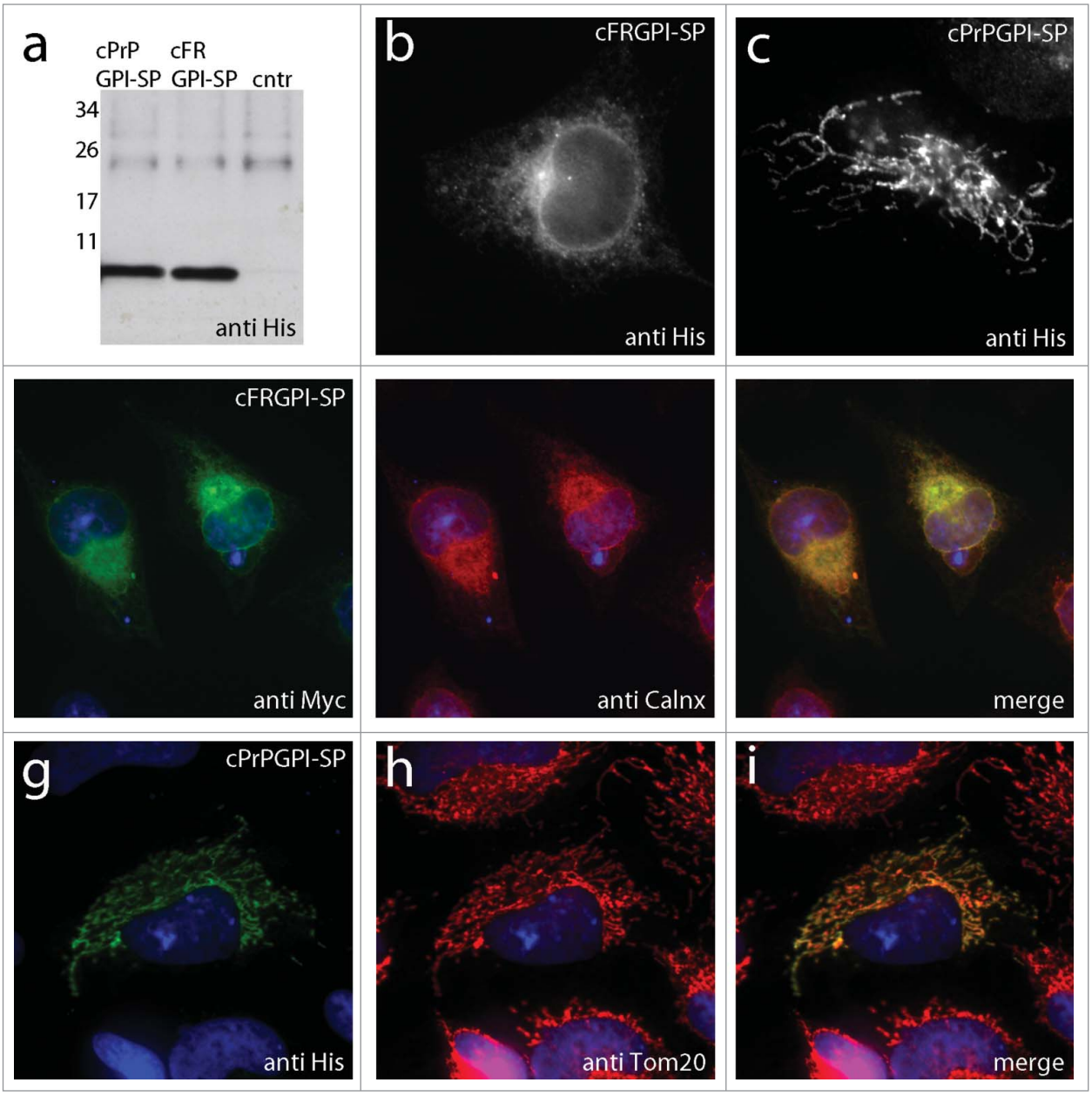

Figure 1. Expression and localization of cPrPGPI-SP and cFRGPI-SP. WB (**a**) and IF (**b, c**) of HeLa cells expressing cFRGPI-SP and cPrPGPI-SP. (**d–f**) colocalization between cFRGPI-SP (green) and the ER marker Calnexin(red). (**g–i**) colocalization between cPrPGPI-SP (green) and the mitochondrial marker Tom20 (red). Nuclei are in blue.

potential (MMP):[34–36] cells were transfected with cPrPGPI-SP and incubated with MitoTracker Red CMXRos (100nM, 30 min) 12h, 24h and 36h after transfection (**Fig. 2a–c** respectively). After fixation, the degree of MMP was visualized qualitatively as red fluorescence while the morphology of nuclei could be observed as blue fluorescence (DAPI staining). Because the uptake of MitoTracker Red depends on MMP, loss in MMP causes a dramatic decrease of red fluorescence. As shown in **Figure 2**, the shape of mitochondria dramatically changed, appearing fragmented at 24h and extensively vacuolarized at 36h after transfection; at the same time the nuclei appeared condensed, a characteristic morphology of cells undergoing apoptosis[37] (**Fig. 2i**). Moreover, the degree of red fluorescence in mitochondria containing cPrPGPI-SP decreased from 12h to 24h and almost completely disappeared 36h after transfection. The degree of colocalization between mitochondria and cPrPGPI-SP was quantified by calculating Manders' overlap coefficient (**Fig. 2j**). Manders' M1 and M2 coefficients measure the portion of the pixels in each channel (here red and green) that coincides with a signal in the other channel. The M coefficient varies from 0 to 1, where 1 indicates complete overlap. After each time-point (12h, 24h, 36h), the value of M1 (amount of

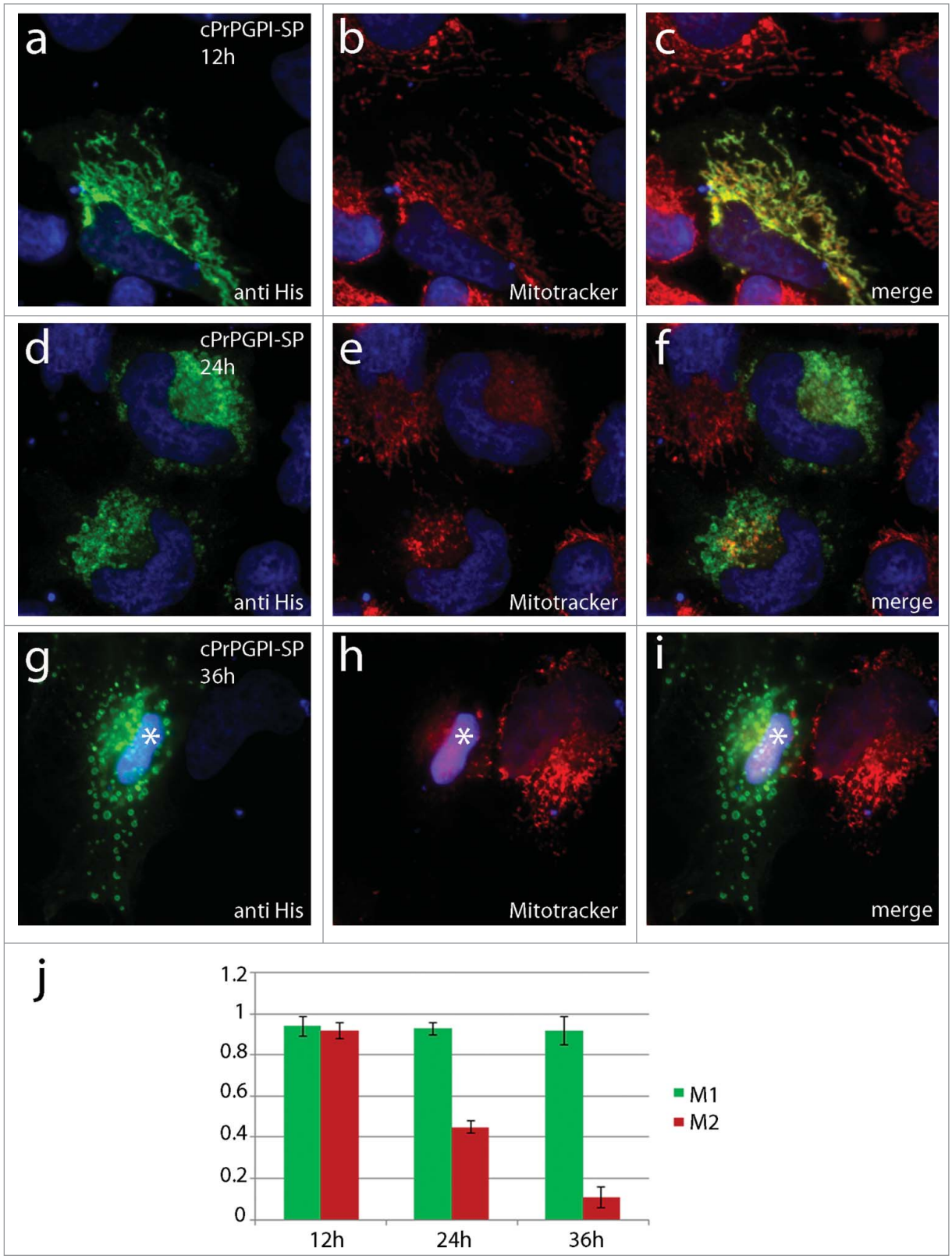

Figure 2. Time course of cPrPGPI-SP expression. HeLa cells transfected with cPrPGPI-SP for 12h (**a–c**), 24h (**d–f**) and 36h (**g–i**) were stained to visualize cPrPGPI-SP (green) and the status of MMP via MitoTracker (red). The absence of red staining indicates loss in MMP. Nuclei are in blue. Asterisk (*) indicates condensed nucleus. Colocalzation efficiency was measured using ImageJ software and shown by Mander's coefficient (**j**). M1 = amount of MitoTracker colocalizing with cPrPGPI-SP; M2 = amount of cPrPGPI-SP colocalizing with MitoTracker. The average and standard deviation were obtained by the analysis of 5 images.

MitoTracker colocalizing with cPrPGPI-SP) was 0.9 ± 0.05, indicating that virtually all Mitotracker signal overlaps with cPrPGPI-SP's signal. However, the value of M2 (amount of cPrPGPI-SP colocalizing with MitoTracker) decreased from 0.9 (at 12h after transfection) to 0.4 and 0.1 (24h and 36h after transfection respectively), indicating that the majority of cPrPGPI-SP had lost MitoTracker staining, which is indicative of loss in MMP.

In conclusion, we were able to show that PrP GPI-SP, when expressed as a cytosolic peptide, is able to localize to the mitochondria and to induce mitochondria fragmentation and vacuolarization, which are accompanied by loss of MMP and ultimately apoptosis. This phenotype of mitochondrial damage and mitochondrial-dependent apoptosis strengthens the evidence that mitochondria play a role in prion pathology. Our results, for the first time, identify the GPI-SP of PrP as a novel candidate responsible for the impairment in mitochondrial function involved in the synaptic pathology observed in prion diseases. It is conceivable that during prion infection PrP GPI-SP may accumulate in the cytoplasm, bind to mitochondria and induce depolarization of the mitochondrial membrane, release of cytochrome c and caspase activation, resulting in neuronal cell death. Further experiments will be necessary to validate this hypothesis in models of prion infection.

Material and Methods

Cells, antibodies and reagents: HeLa cells (obtained from Dr. P. Cossart, Institut Pasteur, Paris, France) were maintained in Dulbecco's modified Eagle's medium (DMEM) (Invitrogen) supplemented with 10% fetal calf serum (FCS) in a 5% CO2 incubator at 37°C. Cells were transfected at 70% confluence using FuGENE6 (Roche Diagnostic) according to manufacturer's protocol. For immunofluorescence and western blot the following antibodies were used: Primary antibodies: rabbit anti-His (a gift from Dr. Dautry, Institut Pasteur); Tom20 (BD Transduction Laboratories, #612278); Calreticulin (Stressgen #SPA-600); Myc9E10 (Sigma #M4439). Secondary antibodies for IF: Alexa fluor 488 goat anti mouse (1:500) and Alexa Fluor 594 goat anti rabbit (1:500) from Molecular Probes. Mitotracker Red CMX Ros (Invitrogen, Carlsbad, CA) was used at a final concentration of 50 nM for 15 min.

DNA constructs: GPI-SPs were inserted into pcDNA3.1MycHis expression vector (Invitrogen) using NheI/BamHI restriction sites. ssGFP-FR-MH and ssGFP-PrP-MH described in[29] were used as templates. Primers: 5'-GGA GAC CCA AGC TGG CTA GCC ACC ATG AAG GAA TTC-3' and BGHRv; the use of a common Fw primer resulted in the addition of 8aa upstream of the omega site.

Immunofluorescence: HeLa cells plated on 12mm glass coverslips were fixed with 4% formaldehyde, permeabilized with 0.1% TritonX100 in PBS for 5 min, then incubated in blocking buffer (PBS containing 10% FCS) for 30 min at room temperature. The cells were then incubated with primary and secondary antibody diluted in blocking buffer. DAPI (Molecular Probes) was used to stain DNA. Coverslips were then mounted onto glass slides with Aqua/Poly Mount (Polysciences) and visualized using a Zeiss Observer Z1 156 inverted microscope with 63× objective controlled by AxioVision software (Zeiss, Thornwood, NY). The degree of colocalization between mitochondria (red) and GA-bodipy (green) was quantified using the colocalization finder and JaCoP plug-in of ImageJ software (http://rsb.info.nih.gov/ij/). Manders' overlap coefficients were measured for at least 5 cells per sample.

Western Blot: Cells were lysed with PAGE loading buffer (60 mM Tris, pH 6.8, 5% 2-mercaptoethanol, 2% SDS, 0.01% Bromophenol blue, and 10% glycerol). Proteins in the lysate were separated by SDS–PAGE using a 4–20% gradient Tris-Tricine gel (Mini-Protean Tris-Tricine Precast Gels, BioRad). Proteins were transferred on Whatman Protran nitrocellulose membranes (0.1um pore size) (Sigma). The membrane was kept in blocking buffer (50 mN, Tris, pH 7.5, 150 mM NaCl, 0.05% Tween 20, and 3% BSA) and then incubated with the primary antibody diluted in blocking buffer. HRP-conjugated secondary antibodies and ECL™ reagents from Amersham (GE Healthcare) were used for detection on Kodak Biomax films.

Disclosure of Potential Conflicts of Interest

No potential conflicts of interest were disclosed.

Funding

The work in C.Z. lab was supported by fellowships from the Federation of European Biochemical Societies (FEBS), the Fondation pour la Recherche Médicale (FRM), the European Union [grant number FP7-KBBE-2007–2A-22287], the ANR (Agence Nationale de la Recherche) (grant numbers ANR-09-BLAN-0122) and the Pasteur–Weizmann Foundation (2010–2012). G.G. gratefully acknowledge Dr. Giulia N. Guizzunti for the critical review of the manuscript.

References

1. Prusiner SB. Prions. Proc Natl Acad Sci USA 1998; 95:13363–83; PMID:9811807; http://dx.doi.org/10.1073/pnas.95.23.13363
2. Cunningham C, Deacon RM, Chan K, Boche D, Rawlins JN, Perry VH. Neuropathologically distinct prion strains give rise to similar temporal profiles of behavioral deficits. Neurobiol Dis 2005; 18:258–69; PMID:15686954; http://dx.doi.org/10.1016/j.nbd.2004.08.015
3. Deacon RM, Raley JM, Perry VH, Rawlins JN. Burrowing into prion disease. Neuroreport 2001; 12:2053–7; PMID:11435945; http://dx.doi.org/10.1097/00001756-200107030-00052
4. Guenther K, Deacon RM, Perry VH, Rawlins JN. Early behavioral changes in scrapie-affected mice and the influence of dapsone. Eur J Neurosci 2001; 14:401–9; PMID:11553290; http://dx.doi.org/10.1046/j.0953-816x.2001.01645.x
5. Cunningham C, Deacon R, Wells H, Boche D, Waters S, Diniz CP, Scott H, Rawlins JN, Perry VH. Synaptic changes characterize early behavioral signs in the ME7 model of murine prion disease. Eur J Neurosci 2003; 17:2147–55; PMID:12786981; http://dx.doi.org/10.1046/j.1460-9568.2003.02662.x
6. Chiesa R, Piccardo P, Dossena S, Nowoslawski L, Roth KA, Ghetti B, Harris DA. Bax deletion prevents neuronal loss but not neurological symptoms in a transgenic model of inherited prion disease. Proc Natl Acad Sci USA 2005; 102:238–43; PMID:15618403; http://dx.doi.org/10.1073/pnas.0406173102
7. Jamieson E, Jeffrey M, Ironside JW, Fraser JR. Apoptosis and dendritic dysfunction precede prion protein accumulation in 87V scrapie. Neuroreport 2001; 12:2147–53; PMID:11447324; http://dx.doi.org/10.1097/00001756-200107200-00021
8. Mallucci GR. Prion neurodegeneration: starts and stops at the synapse. Prion 2009 3:195–201; PMID:19887910; http://dx.doi.org/10.4161/pri.3.4.9981
9. Sisková Z, Mahad DJ, Pudney C, Campbell G, Cadogan M, Asuni A, O'Connor V, Perry VH. Morphological and functional abnormalities in mitochondria associated with synaptic degeneration in prion disease.

Am J Pathol 2010; 177:1411–21; PMID:20651247; http://dx.doi.org/10.2353/ajpath.2010.091037
10. Li Z, Okamoto K, Hayashi Y, Sheng M: The importance of dendritic mitochondria in the morphogenesis and plasticity of spines and synapses. Cell 2004; 119:873–87; PMID:15607982; http://dx.doi.org/10.1016/j.cell.2004.11.003
11. Trimmer PA, Swerdlow RH, Parks JK, Keeney P, Bennett JP, Jr., Miller SW, Davis RE, Parker WD, Jr. Abnormal mitochondrial morphology in sporadic Parkinson's and Alzheimer's disease cybrid cell lines. Exp Neurol 2000; 162:37–50; PMID:10716887; http://dx.doi.org/10.1006/exnr.2000.7333
12. Castellani R, Hirai K, Aliev G, Drew KL, Nunomura A, Takeda A, Cash AD, Obrenovich ME, Perry G, Smith MA. Role of mitochondrial dysfunction in Alzheimer's disease. J Neurosci Res 2002; 70:357–60; PMID:12391597; http://dx.doi.org/10.1002/jnr.10389
13. Dawson TM, Dawson VL. Molecular pathways of neurodegeneration in Parkinson's disease. Science 2003; 302:819–22; PMID:14593166; http://dx.doi.org/10.1126/science.1087753
14. Beal MF. Mitochondria take center stage in aging and neurodegeneration. Ann Neurol 2005; 58:495–505; PMID:16178023; http://dx.doi.org/10.1002/ana.20624
15. Grenier C, Bissonnette C, Volkov L, Roucou X. Molecular morphology and toxicity of cytoplasmic prion protein aggregates in neuronal and non-neuronal cells. J Neurochem 2006; 97:1456–66; PMID:16696854; http://dx.doi.org/10.1111/j.1471-4159.2006.03837.x
16. Mattei V, Matarrese P, Garofalo T, Tinari A, Gambardella L, Ciarlo L, Manganelli V, Tasciotti V, Misasi R, Malorni W, et al. Recruitment of cellular prion protein to mitochondrial raft-like microdomains contributes to apoptosis execution. Mol Biol Cell 2011 22:4842–53; PMID:22031292; http://dx.doi.org/10.1091/mbc.E11-04-0348
17. Hachiya NS, Yamada M, Watanabe K, Jozuka A, Ohkubo T, Sano K, Takeuchi Y, Kozuka Y, Sakasegawa Y, Kaneko K. Mitochondrial localization of cellular prion protein (PrPC) invokes neuronal apoptosis in aged transgenic mice overexpressing PrPC. Neurosci Lett 2005; 374:98–103; PMID:15644272; http://dx.doi.org/10.1016/j.neulet.2004.10.044
18. Wang X, Dong CF, Shi Q, Shi S, Wang GR, Lei YJ, Xu K, An R, Chen JM, Jiang HY, et al. Cytosolic prion protein induces apoptosis in human neuronal cell SH-SY5Y via mitochondrial disruption pathway. BMB Rep 2009; 42:444–9; PMID:19643043; http://dx.doi.org/10.5483/BMBRep.2009.42.7.444
19. Carimalo J, Cronier S, Petit G, Peyrin JM, Boukhtouche F, Arbez N, Lemaigre-Dubreuil Y, Brugg B, Miquel MC. Activation of the JNK-c-Jun pathway during the early phase of neuronal apoptosis induced by PrP106-126 and prion infection. Eur J Neurosci 2005; 21:2311–9; PMID:15932590; http://dx.doi.org/10.1111/j.1460-9568.2005.04080.x
20. O'Donovan CN, Tobin D, Cotter TG. Prion protein fragment PrP-(106-126) induces apoptosis via mitochondrial disruption in human neuronal SH-SY5Y cells. J Biol Chem 2001; 276:43516–23; PMID:11533027; http://dx.doi.org/10.1074/jbc.M103894200
21. Dupiereux I, Zorzi W, Rachidi W, Zorzi D, Pierard O, Lhereux B, Heinen E, Elmoualij B. Study on the toxic mechanism of prion protein peptide 106-126 in neuronal and non neuronal cells. J Neurosci Res 2006; 84:637–46; PMID:16786576; http://dx.doi.org/10.1002/jnr.20965
22. Crozet C, Beranger F, Lehmann S. Cellular pathogenesis in prion diseases. Vet Res; 2008 39:44; PMID:18413130; http://dx.doi.org/10.1051/vetres:2008021
23. Stahl N, Borchelt DR, Hsiao K, Prusiner SB. Scrapie prion protein contains a phosphatidylinositol glycolipid. Cell 1987; 51:229–40; PMID:2444340; http://dx.doi.org/10.1016/0092-8674(87)90150-4
24. Orlean P, Menon AK. GPI anchoring of protein in yeast and mammalian cells, or: how we learned to stop worrying and love glycophospholipids. J Lipid Res 2007; 48:993–1011; PMID:17361015; http://dx.doi.org/10.1194/jlr.R700002-JLR200
25. Ohishi K, Inoue N, Kinoshita T. PIG-S and PIG-T, essential for GPI anchor attachment to proteins, form a complex with GAA1 and GPI8. EMBO J 2001; 20:4088–98; PMID:11483512; http://dx.doi.org/10.1093/emboj/20.15.4088
26. Caras IW. Probing the signal for glycophosphatidylinositol anchor attachment using decay accelerating factor as a model system. Cell Biol Int Rep 1991; 15(9):815–26; PMID:1724950; http://dx.doi.org/10.1016/0309-1651(91)90035-H
27. Hoque MZ, Kitamoto T, Furukawa H, Muramoto T, Tateishi J. Mutation in the prion protein gene at codon 232 in Japanese patients with Creutzfeldt–Jakob disease: a clinicopathological, immunohistochemical and transmission study. Acta Neuropathol 1996; 92:441–6; PMID:8922054; http://dx.doi.org/10.1007/s004010050544
28. Windl O, Giese A, Schulz-Schaeffer W, Zerr I, Skworc K, Arendt S, Oberdieck C, Bodemer M, Poser S, Kretzschmar HA. Molecular genetics of human prion diseases in Germany. Hum Genet 1999; 105:244–52; PMID:10987652; http://dx.doi.org/10.1007/s004390051096
29. Guizzunti G, Zurzolo C. The fate of PrP GPI-anchor signal peptide is modulated by P238S pathogenic mutation. Traffic 2014; 15:78–93; PMID:24112521; http://dx.doi.org/10.1111/tra.12126
30. Sommer T, Jentsch S. A protein translocation defect linked to ubiquitin conjugation at the endoplasmic reticulum. Nature 1993; 365:176–9; PMID:8396728; http://dx.doi.org/10.1038/365176a0
31. Rodighiero C, Tsai B, Rapoport TA, Lencer WI. Role of ubiquitination in retro-translocation of cholera toxin and escape of cytosolic degradation. EMBO Rep 2002; 3:1222–7; PMID:12446567; http://dx.doi.org/10.1093/embo-reports/kvf239
32. de Virgilio M, Weninger H, Ivessa NE. Ubiquitination is required for the retro-translocation of a short-lived luminal endoplasmic reticulum glycoprotein to the cytosol for degradation by the proteasome. J Biol Chem 1998 273:9734–43; PMID:9545309; http://dx.doi.org/10.1074/jbc.273.16.9734
33. Gu Y, Singh A, Bose S, Singh N. Pathogenic mutations in the glycosylphosphatidylinositol signal peptide of PrP modulate its topology in neuroblastoma cells. Mol Cell Neurosci 2008; 37:647–56; PMID:18325785; http://dx.doi.org/10.1016/j.mcn.2007.08.018
34. Susin SA, Lorenzo HK, Zamzami N, Marzo I, Snow BE, Brothers GM, Mangion J, Jacotot E, Costantini P, Loeffler M, et al. Molecular characterization of mitochondrial apoptosis-inducing factor. Nature 1999; 397:441–6; PMID:9989411; http://dx.doi.org/10.1038/17135
35. Haugland RP. Molecular Probes: Handbook of Fluorescent Probes and Research Chemicals, 6th Ed., pp. 266–267. Eugene, OR: Molecular Probes, Inc.; 1996
36. Poot M, Zhang YZ, Kramer JA, Wells KS, Jones L, Hanzel DK, Lugade AG, Singer VL, Haughland RP. Analysis of mitochondrial morphology and function with novel fixable fluorescent stains. J Histochem Cytochem 1996; 44:1363–72; PMID:8985128; http://dx.doi.org/10.1177/44.12.8985128
37. Johnson VL, Ko SC, Holmstrom TH, Eriksson JE, Chow SC. Effector caspases are dispensable for the early nuclear morphological changes during chemical-induced apoptosis. J Cell Sci 2000 113:2941–53; PMID:10934034